Aptamer-Nanoparticle Assembly for Logic-Based Detection

Mohammed I. Shukoor, Meghan O. Altman, Da Han, Abdullah Tahir Bayrac, Ismail Ocsoy, Zhi Zhu and Weihong Tan*

Supporting Information

Table S1. List of sequences with modifications used in experiments.

Probe	(Dye)-(Extension)-Sequence (5'→3')
PDGF-aptamer	(TAMRA)-(CTCAG)-CAGGCTACGGCAC GTAGAGCATCACCATGATCCTG
VEGF-aptamer	(FITC)-(TATCC)-CCGTCTTCCAGACAAG AGTGCAGGG
PDGF-mutant	(TAMRA)-(CTCAG)-CAGGCTGCACATACTCACTTACTACTATGTCCATA
VEGF-mutant	(FITC)-(TATCC)-CCCGTCTACCCTTCTCAATGTTATTG
P-SH	AGCCTG CTGAG TATCC TTTTT
V-SH	AGACGG GGATA CTCAG TTTTT

Figure S2 shows the UV/Vis spectra of 3'-SH-20mer carrier strand modified Au nanoparticles. (a) Au $_{P\text{-}SH}$ and (b) Au $_{V\text{-}SH}$ show only a slight shift in the plasmon band (525 nm) from 520 nm for unmodified Au nanoparticles (not shown). The differences in their absorption peaks may result from the fabrication process during DNA modification of Au nanoparticles [2]. (c) Hybridization between the complementary Au nanoparticle system causes large three-dimensional aggregates which leads to a red shift in the surface plasmon resonance from λ_{max} = 525 to 560 nm.

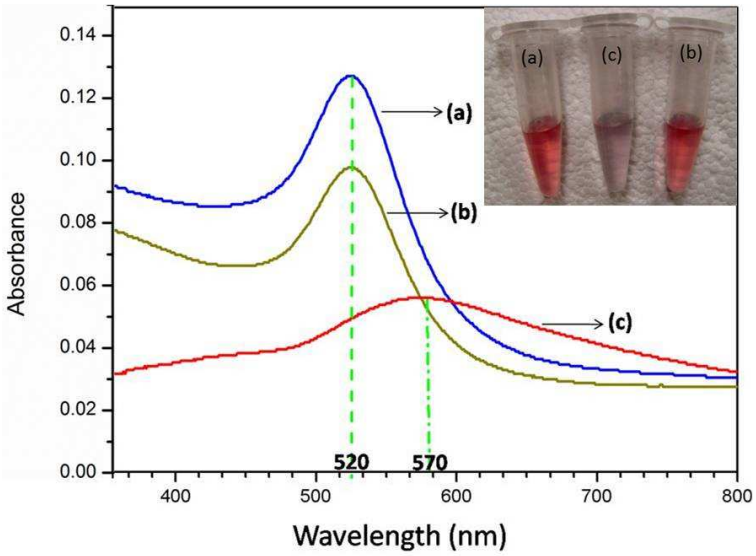

Figure S2. The UV/Vis spectra of (a) Au $_{P\text{-}SH}$ and (b) Au $_{V\text{-}SH}$ DNA modified and (c) a hybridization mixture of both types of Au nanoparticles.

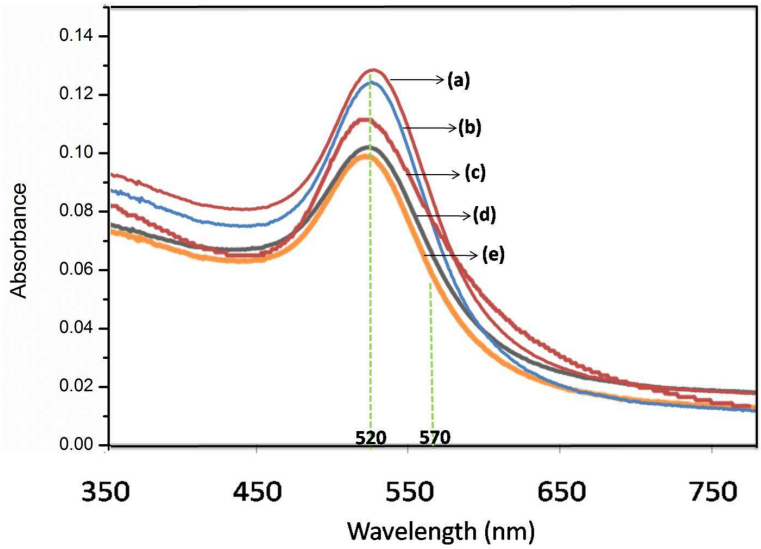

Figure S3. Cross talks. The UV/Vis spectra of (a) Au $_{PDGF\ aptamer/P\text{-}SH}$, (b) Au $_{VEGF\ aptamer/V\text{-}SH}$, (c) Au $_{PDGF\ aptamer/P\text{-}SH}$ + Au $_{V\text{-}SH}$, (d) Au $_{VEGF\ aptamer/V\text{-}SH}$ + Au $_{P\text{-}SH}$, and (e) Au $_{PDGF\ aptamer/P\text{-}SH}$ + Au $_{VEGF\ aptamer/V\text{-}SH}$ modified Au nanoparticles.

Various controls were performed to ensure no crosstalk or self-hybridization between probes which may lead to aggregate formation. UV/Vis spectra (Fig S3) of (a) Au $_{PDGF\ aptamer/P\text{-}SH}$, (b) Au $_{VEGF\ aptamer/V\text{-}SH}$, (c) Au $_{PDGF\ aptamer/P\text{-}SH}$ + Au $_{V\text{-}SH}$, (d) Au $_{VEGF\ aptamer/V\text{-}SH}$ + Au $_{P\text{-}SH}$, and (e) Au $_{PDGF\ aptamer/P\text{-}SH}$ + Au $_{VEGF\ aptamer/V\text{-}SH}$ modified Au nanoparticles show no characteristic broadening of the surface plasmon peak.

Two sets of control experiments were performed to confirm that nanoparticle agglomeration is an outcome of specific binding of aptamers to their respective target proteins (Table S4). (i) **Control proteins;** Lysozyme (100 nM) and BSA (Bovine Serum Albumin, 100 nM) were used as control proteins for aptamer-nanoparticle probes (Au $_{\text{TAMRA-PDGF-aptamer-/P-SH}}$ and Au $_{\text{FITC-VEGF-aptamer-/V-SH}}$ (Table S4, samples **b** and **c**). **(ii) Mutant sequences;** Two 5'-Dye - modified mutant strands partially complementary to their respective carrier strands conjugated with the nanoparticles (Au $_{\text{TAMRA-mutant1-/P-SH}}$ and Au $_{\text{FITC-mutant2/V-SH}}$) were used in combination with aptamer-nanoparticle probes (Table S4, samples **d** and **e**). All sequences of the carrier strands were kept the same as described in **Scheme 1.** Samples **a** and **f** (Table S4) correspond to pure aptamer-nanoparticle and mutant-nanoparticle complex, respectively, with no target or control proteins added. Sample **g** (Table S4) consists of aptamer-nanoparticle complex in the presence of target proteins (PDGF and VEGF) as positive control.

Table S4: Various input conditions followed during the control experiments

Sample	Probes	Target
a	Au $_{\text{TAMRA-PDGF-aptamer-/P-SH}}$ Au $_{\text{FITC-VEGF-aptamer-/V-SH}}$	-
b	Au $_{\text{TAMRA-PDGF-aptamer-/P-SH}}$ Au $_{\text{FITC-VEGF-aptamer-/V-SH}}$	BSA
c	Au $_{\text{TAMRA-PDGF-aptamer-/P-SH}}$ Au $_{\text{FITC-VEGF-aptamer-/V-SH}}$	Lysozyme
d	Au $_{\text{TAMRA-mutant1-/P-SH}}$ Au $_{\text{FITC-VEGF-aptamer-/V-SH}}$	PDGF
e	Au $_{\text{TAMRA-PDGF aptamer-/P-SH}}$ Au $_{\text{FITC-mutant2-/V-SH}}$	VEGF
f	Au $_{\text{TAMRA-mutant1-/P-SH}}$ Au $_{\text{FITC-mutant2-/V-SH}}$	-
g	Au $_{\text{TAMRA-PDGF aptamer-/P-SH}}$ Au $_{\text{FITC-VEGF-aptamer-/V-SH}}$	PDGF, VEGF

Figure S5 (**A**) shows visual detection of samples **a-g**, as described in Table S4. The PDGF and VEGF aptamer-probes show no non-specific binding towards BSA or lysozyme and the nanoparticle solution remains red (Fig. S5 **A** (**b**) and (**c**), Supporting info). Similar results were obtained for a mixture of mutant- and aptamer- nanoparticle probes in the presence of PDGF (Fig. S5 **A**, (**d**), Supporting info) and VEGF (Fig. S5 **A** (**e**), Supporting info), respectively, where no color change was observed. Moreover, the hybridization of aptamer and mutant sequences with their respective carrier strands on the Au nanoparticle system remained stable for more than two weeks and caused no color change (Fig. S5 **A**, (**a**) and (**f**), Supporting info). Color change from red to violet is observed only for sample **g** consisting of both types of aptamer-nanoparticles in the presence of both PDGF and VEGF

proteins (Fig. S5 **A** (**g**)**,** Supporting info). Figure S5 (**B**) **(**Supporting info**)** shows fluorescence intensities (blue bar: FITC and red bar: TAMRA) for samples **a-g** in response to protein inputs. No restoration of fluorescence signal was observed in the presence of control proteins or mutant aptamers, because the dye-tagged aptamers/mutants remained attached to the carrier strands and fluorescence was quenched due to the Au nanoparticles. Only sample **g** (Fig. S5 **B** (**g**), Supporting info) shows both FITC (VEGF-aptamer, blue bar) and TAMRA (PDGF-aptamer, red bar) signals when incubated with a mixture of PDGF and VEGF proteins indicating that the fluorescence recovery was due mainly to the duplex dissociation induced by specific binding between aptamers and target proteins.

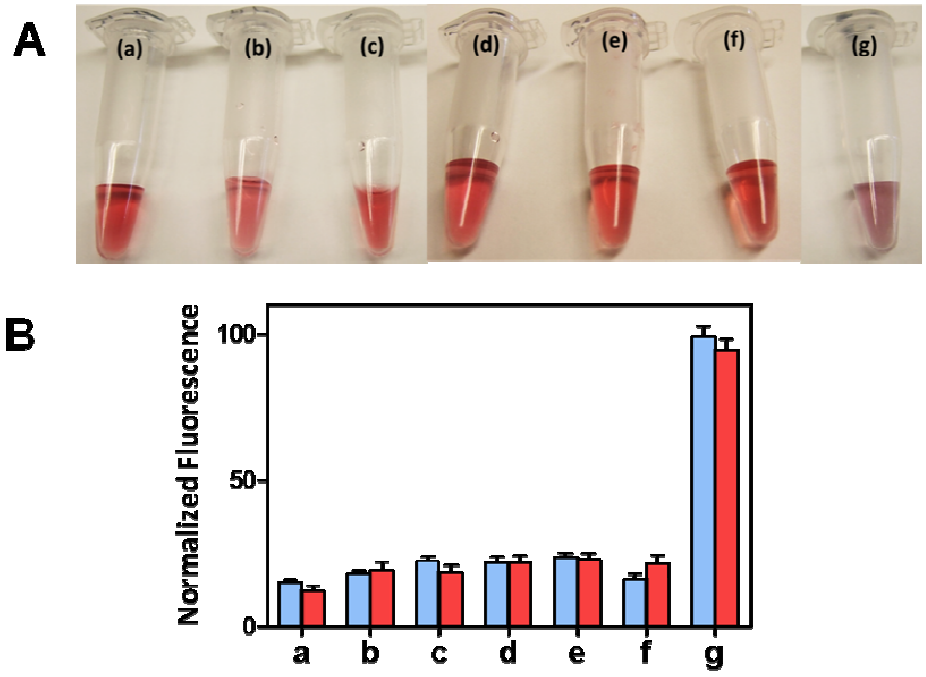

Figure S5. (A) Colorimetric and **(B)** fluorescence detection of samples described in Table S4.

Additionally, the UV/Vis spectra for samples **a-c** (Fig. S6 (**A**), Supporting Info) and samples **d-f** (Fig. S6 (**B**), Supporting Info) show no broadening of the Au nanoparticle absorption maximum.

Nanoparticle aggregation and dispersion was further confirmed using TEM (Fig. S7, Supporting Info). Figure S7 (**A**), (**B**), and (**C**) correspond to samples **a, b** and **d** respectively, where no aggregation was observed. The aggregation of Au nanoparticles was observed only in sample **g** (Fig. S7 (**D**), Supporting info).

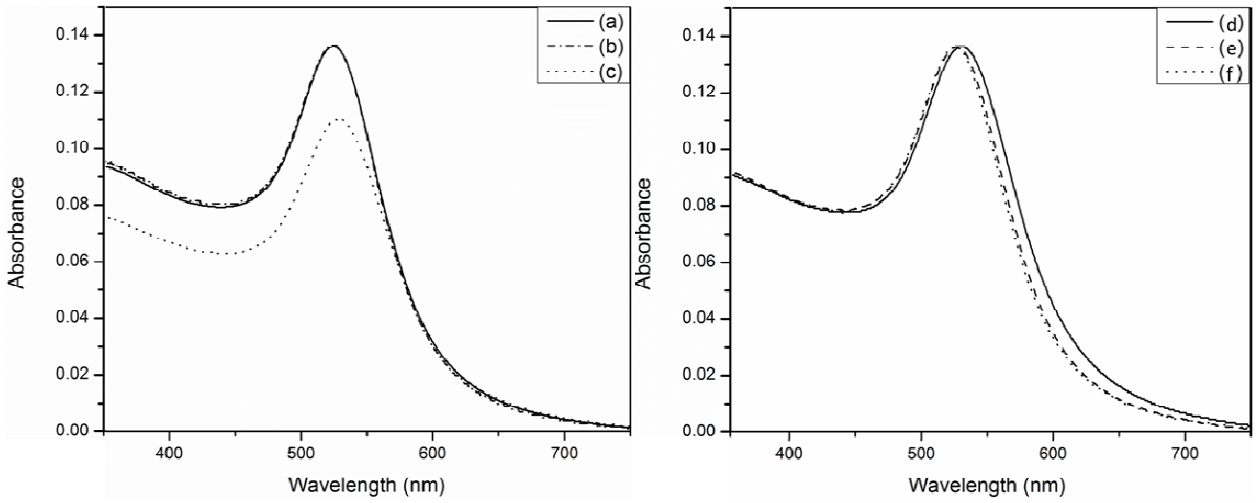

Figure S6. The UV/Vis spectra of control experiments/samples **a-f** described in Table S4.

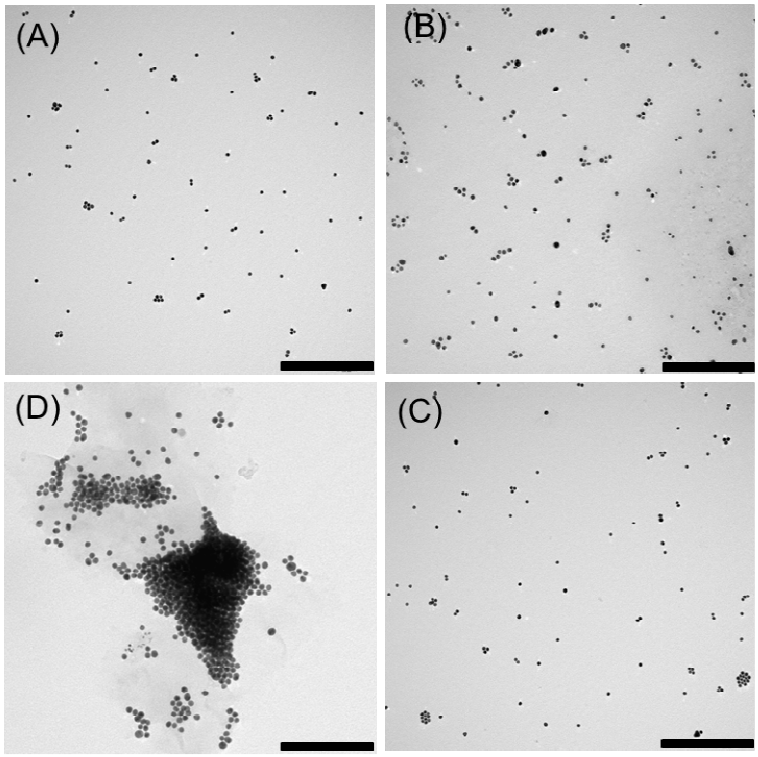

Figure S7. TEM images of control experiments/samples (A) **a**, (B) **b**, (C) **d** and (D) **g** as described in Table S4. (scale bar 200 nm)